

Effect of Annealing on the Optical Properties of $\text{AgGa}_{0.5}\text{In}_{0.5}\text{Te}_2$ Thin Film

G. B. Sakr ^{*1} and E. A. El-Sayad ²

¹ Physics Department, Faculty of Education, Ain Shams Univ.,
Cairo, Egypt

² Solid State Physics Department, Physics Division, National Research
Centre, Dokki, Cairo, Egypt

AgGa_{0.5}In_{0.5}Te₂ thin films were deposited, by thermal evaporation of presynthesised bulk ingot material, onto a Corning 7095 glass substrates. EDXS studies on the prepared films show that the as-deposited films are nearly stoichiometric. Also, XRD studies on the as-deposited and annealed films revealed an amorphous-to-crystalline phase transition at $T_a \approx 473$ K. The optical constants (n , k) of the amorphous and crystalline $\text{AgGa}_{0.5}\text{In}_{0.5}\text{Te}_2$ films, were determined from the transmittance and the reflectance data at normal incidence in the spectral range 400-2500 nm. The high frequency dielectric constant and the carrier concentration and the effective mass ratio were determined from the analysis of the refractive index at long wavelengths. The analysis of the absorption spectra of the investigated films revealed non-direct energy gaps, characterizing the amorphous films, in contrary to the crystalline films which exhibited only direct energy gaps.

1. Introduction:

The I-III-VI₂ ternary semiconducting compounds are the isoelectronic analogue of II-VI binary compound semiconductors and they crystallize in the tetragonal chalcopyrite structure with space group $\bar{1}42d$ [1]. They have received considerable attention because of their potential application in photovoltaic cells, optoelectronic devices and non-linear optical systems [2-4]. The broad range of optical, electrical, and structural properties offered by the I-III-VI₂ ternary semiconductors, as well as their ability to form various solid solutions and to accommodate different dopants, has led to their emergence as technologically significant device materials and represent promising alternative

* Corresponding author, e-mail: gamalsaker@yahoo.com

to those currently employed in device fabrication [1, 5]. By making suitable solid solutions among them [6–8], it is possible to obtain a new alloy with specific characteristics to meet a desired requirement.

Among the several materials of this group, AgInTe₂ and AgGaTe₂ have proved to be effective and stable light absorbers for the fabrication of heterojunction solar cells and infrared light sources [2, 3]. The two compounds are direct band gap semiconductors showing a three-fold optical structure near the fundamental absorption edge [1, 4]. These compounds have been widely studied in both bulk and thin film form; however, very little information about their solid solutions was reported.

The stoichiometric bulk ingot material of AgGa_{0.5}In_{0.5}Te₂ as well as that thermally evaporated films has been previously prepared by one of the authors [8]. The structural characterization of the bulk material as well as the deposited films was investigated in details. The author reported that the as-deposited and annealed films at 373, 423 K for 1 h are amorphous, while those annealed at 473 and 523 K are polycrystalline with single-phase of a tetragonal chalcopyrite structure. Analysis of the optical absorption spectrum of the polycrystalline films revealed three energy gaps viz. 1.142, 1.213 and 1.907 eV, which were attributed to the fundamental, band splitting by crystal-field and spin-orbit effects, respectively [8].

Since evaluation of the optical absorption and refractive indices of such materials are of considerable importance for applications in integrated optical devices, so it is necessary to study the effect of annealing temperature on the optical properties of the deposited AgGa_{0.5}In_{0.5}Te₂ amorphous thin films.

2. Experimental Procedures:

High quality thin films of AgGa_{0.5}In_{0.5}Te₂ were prepared by thermal evaporation of the presynthesised and checked bulk material [8] onto pre-cleaned Corning 7095 glass substrates held at room temperature (300 K), in a vacuum of $\sim 5 \times 10^{-4}$ Pa, using a high- vacuum coating unit (Edwards 306 A). The deposition rate was kept constant during the evaporation process at nearly 5 nm/s. The film thickness, t , was monitored using a quartz crystal thickness monitor (Edwards, FTM4) and it was also measured interferometrically [9]. Differential thermal analysis of the prepared powder was carried out using Shimatzu DSC 50 with 10K/min. The as-deposited films were annealed at $T_a = 373, 423, 473, \text{ and } 523$ K for 1 h in a vacuum of $\sim 1.5 \times 10^{-1}$ Pa.

The elemental composition of the as-deposited films was determined using an energy-dispersive X-ray spectrometer (EDXS) unit, interfaced with a scanning electron microscope (SEM; Philips XL) operating at an accelerating voltage of 30 kV. X-ray diffractograms of the investigated films were carried out at 300 K using an automatic X-ray diffractometer (Philips Type X'Pert) with Ni-filtered, CuK_α ($\lambda_1 = 1.54056 \text{ \AA}$) radiation operated at 30 mA and 40 kV.

The optical transmittance, T , and reflectance, R , of the as-deposited and annealed films were recorded at room temperature with unpolarized light at normal incidence in the wavelength range of 400-2500 nm using a double beam spectrophotometer (JASCO Corp., model V-570).

3. Results and Discussions:

EDXS analysis of the bulk $\text{AgGa}_{0.5}\text{In}_{0.5}\text{Te}_2$ material as well as the corresponding as-deposited films confirms the presence of the indicated elements with exact nominal chemical composition of $\text{Ag}_{0.987}\text{Ga}_{0.545}\text{In}_{0.546}\text{Te}_{1.922}$ and $\text{Ag}_{0.933}\text{Ga}_{0.522}\text{In}_{0.546}\text{Te}_{2.035}$, respectively. The EDXS analysis data of $\text{AgGa}_{0.5}\text{In}_{0.5}\text{Te}_2$ compound in powder form and thin film form compared to the calculated one are summarized in Table (1).

Table 1: EDAX analysis data of $\text{AgGa}_{0.5}\text{In}_{0.5}\text{Te}_2$ compound in powder and thin film form compared to the calculated one.

Element	Elemental composition at. %		
	Bulk (obs.)	Thin film (obs.)	Calculated
Ag	24.67	23.33	25.0
Ga	13.63	13.06	12.5
In	13.66	12.73	12.5
Te	48.04	50.88	50.0

XRD studies revealed that the as-deposited films as well as those annealed at $T_a = 373$ and 423 K are amorphous in nature, while those annealed at $T_a = 473$ and 523 K are polycrystalline with a preferred orientation plane (112) parallel to the substrate (Fig. 1). This result is in consistent with the DTA (not shown); in which an endothermic peak located at temperature 480 K, indicates an onset of phase transformation begins to occur. Similar result was also observed for the quaternary CdGaInSe_4 [10]. The phase transformation has been already observed from the DTA analysis of some $A^I B^{III} C_2^{VI}$ chalcopyrite compounds including the ternary AgGaTe_2 and AgInTe_2 single crystal and explained due to irreversible volume change [11].

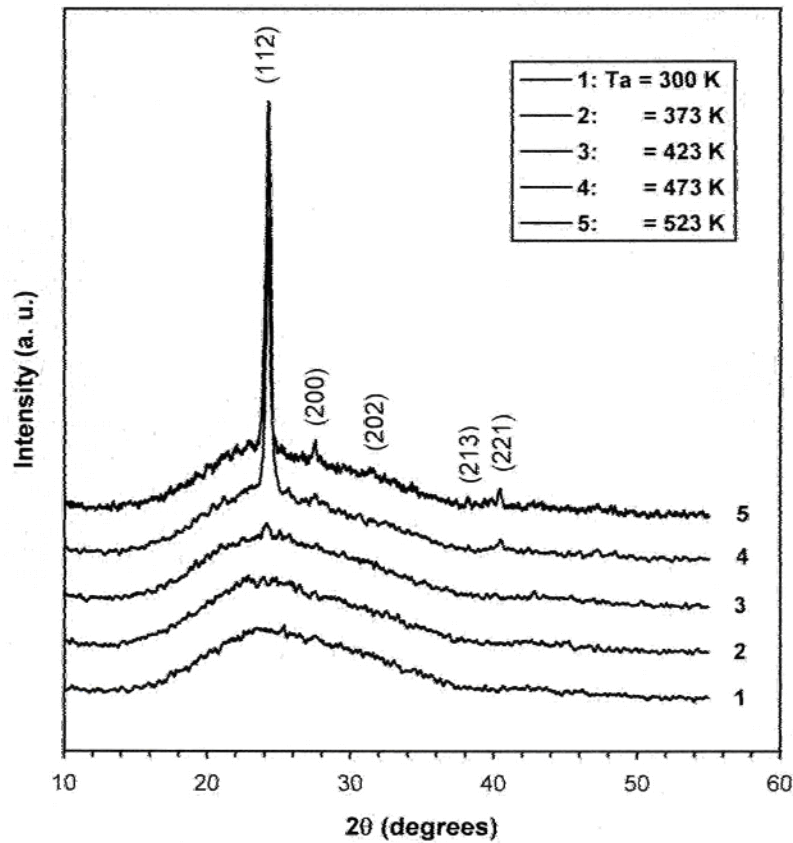


Fig. (1): Observed X-ray diffractograms of as-deposited and annealed AgGa_{0.5}In_{0.5}Te₂ films: (1) as-deposited; (2) T_a = 373, (3) 423, (4) 473, and (5) 523 K. (cited as Fig.1b in Ref.8).

Figure (2) shows the transmission, T , and reflection, R , spectra at normal light incidence in the wavelength range 300–2500 nm for as-deposited film and those after being annealed at 373, 423, 473 and 523 K. From the transmittance spectrum one can see a blue shift of the short wavelength absorption edge with increasing annealing temperature up to 423 K, however with further increasing of the annealing temperature > 423 K a red shift of short wavelength absorption edge has been observed. Furthermore, beyond the absorption edge, the transmission spectrum of the investigated samples improves significantly with annealing temperature over the whole studied wavelength range.

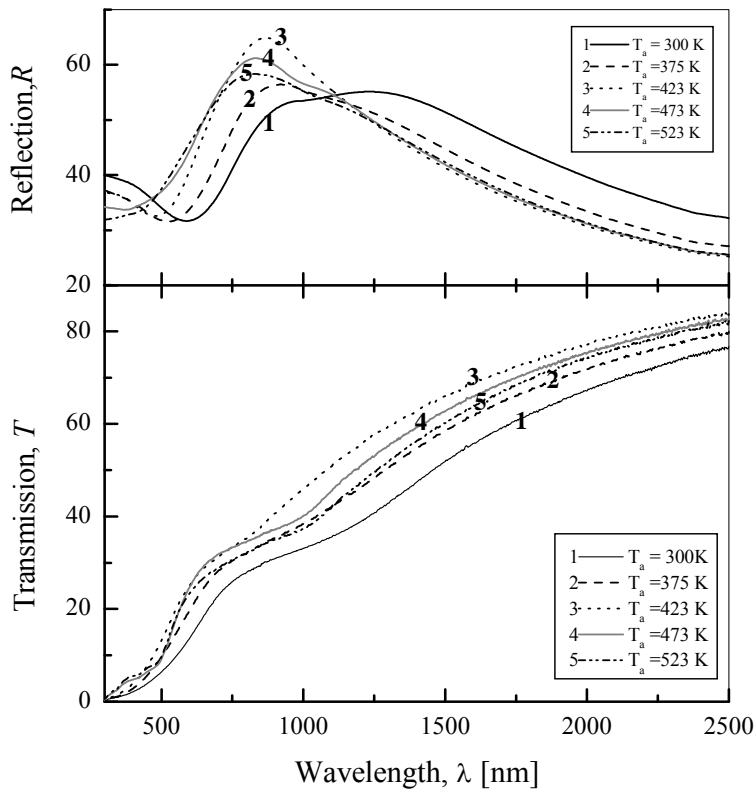


Fig. (2): Transmission, T and reflection, R spectrum for as-deposited and annealed $\text{AgGa}_{0.5}\text{In}_{0.5}\text{Te}_2$ films.

The optical constants (n & k) for both the as-deposited and annealed films were determined from both the measured values of T and R (after correcting for the absorptance and reflectance of the substrate) using a simple computer program. The optical absorption coefficient, α could be calculated from the values of T and R [12, 13] using the following relation;

$$\alpha = \frac{1}{t} [\ln(C + \sqrt{C^2 + R^2})] \tag{1}$$

where t is the film thickness, $C = (1-R)^2/2T$. The refractive index, n , could be determined from the values of R and the determined values of the extinction coefficient, k ($=\alpha\lambda/4\pi$), using the relation [12, 13];

$$n = \sqrt{N^2 - k^2} \tag{2}$$

$$N = (1 + \sqrt{R}) / (1 - \sqrt{R}) \quad (3)$$

where $N (= n + ik)$ is the complex refractive index. Taking into account the experimental error in measuring the film thickness to be $\pm 2\%$ and in T and R to be 0.5% , the error of the adopted technique in the calculated values of n and k was estimated to be 1.1% and 0.5% , respectively. The optical constants n and k were found to be independent of the film thickness in the investigated range, where a wide change in t gives a minute change in both n and k .

Figure (3) gives the spectral distribution of the refractive index, n , of the as-deposited and annealed films showing how n depending on the annealing temperature. However, it was observed that in the low wavelength range ($500 \leq \lambda \leq 1300$ nm) the refractive index, n , shows anomalous dispersion, and the value of n increases with increasing T_a for the amorphous films at certain λ , while for the polycrystalline films n decreases as T_a increases and exhibit a slightly lower value than those annealed at 423 K. It could also be observed that in the long wavelength range ($900 \leq \lambda \leq 2500$ nm) n decreases monotonically, and the value of n decreases with increasing T_a for the amorphous films at certain λ , while for the polycrystalline films n increases as T_a increases and exhibit a slightly lower value than those annealed at 423 K. The behaviour of n of the films annealed at 473 and 523 K indicates that such films are completely crystallized.

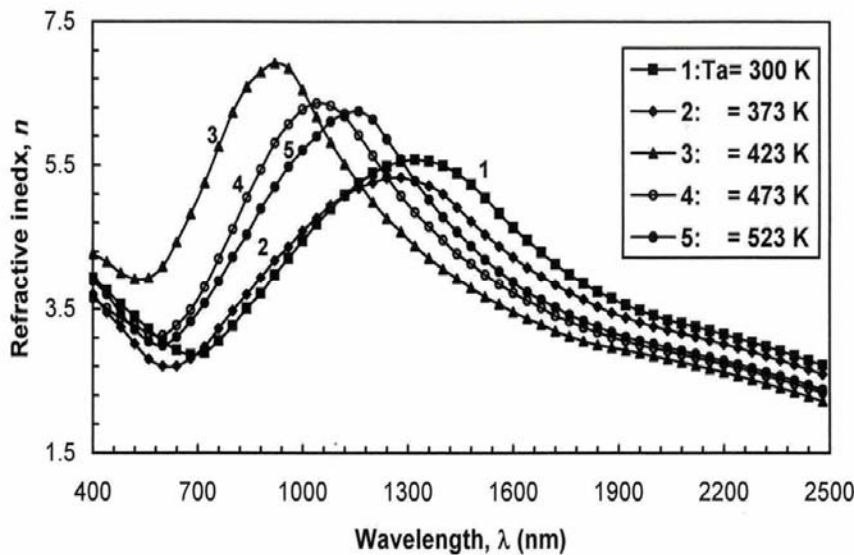


Fig. (3): Spectral distribution of the refractive index, n , for as-deposited and annealed $\text{AgGa}_{0.5}\text{In}_{0.5}\text{Te}_2$ films.

The decrease in the value of n with increasing λ in the long wavelengths may be attributed to the effect of the free carrier concentration. So, a plot of $\epsilon_r = n^2 - k^2$, versus λ^2 (Fig. 4) for long wavelengths exhibits a straight line in accordance with the relation [14],

$$\epsilon_r = \epsilon_\infty - (e^2 / 4\pi^2 c^2 \epsilon_0)(N / m^*)\lambda^2 \tag{4}$$

where $\epsilon_\infty = n_\infty^2$, e is the electronic charge, c is the speed of light, ϵ_0 is the permittivity of free space, N/m is the charge carrier concentration to the effective mass ratio. The high frequency dielectric constants, ϵ_∞ , and the ratio N/m , could be deduced from the intercept and the slope of the straight line (Table 2).

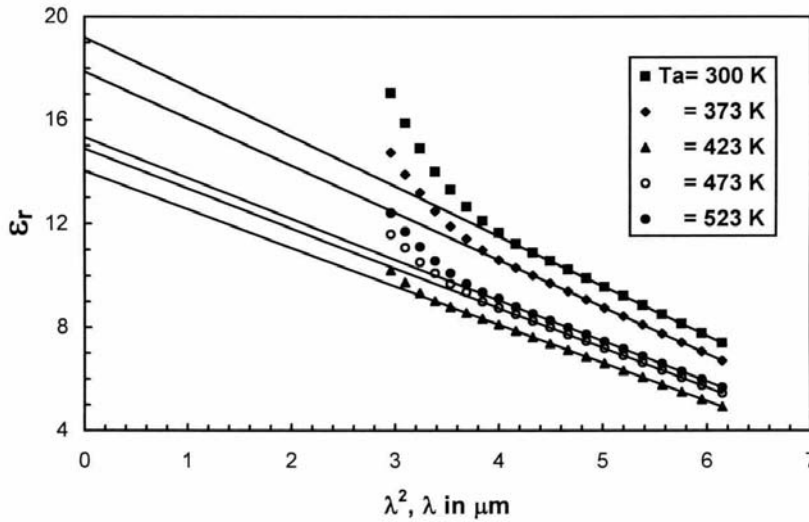


Fig. (4): Plot of ϵ_r versus λ^2 for the indicated samples.

Table 2: The optical parameters of the as-deposited and annealed $\text{AgGa}_{0.5}\text{In}_{0.5}\text{Te}_2$ films.

T_a (K)	ϵ_∞	$N/m \times 10^{-21}$ (cm^{-3})	E_g (eV)	E_{g2} (eV)	E_{g3} (eV)
300	19.202	2.140	0.754	-----	-----
373	17.869	2.023	0.838	-----	-----
423	14.042	1.653	1.236	-----	-----
473	14.896	1.712	1.156	1.316	1.99
523	15.337	1.752	1.117	1.255	1.93
523*	-----	-----	1.142	1.213	1.907

* Previously reported data [8].

The spectral behaviour of the absorption coefficient, α , (Fig. 5) represents typical curves showing the dependence of α on photon energy, $h\nu$, and the annealing temperature, T_a . The analysis of the absorption coefficients of the amorphous films (Fig. 5) was found to follow the relation;

$$\alpha(h\nu) = (A/h\nu)(h\nu - E_g)^p \quad (5)$$

with $p = 2$, which characterizes a non-direct optical transition for the amorphous films according to Tauc [15]. A plot of $(\alpha h\nu)^{1/2}$ versus $h\nu$ yields a straight line for the as-deposited samples and the films annealed at 373, and 423 K (Fig. 6) with $E_g = 0.754, 0.838, \text{ and } 1.236$ eV, respectively.

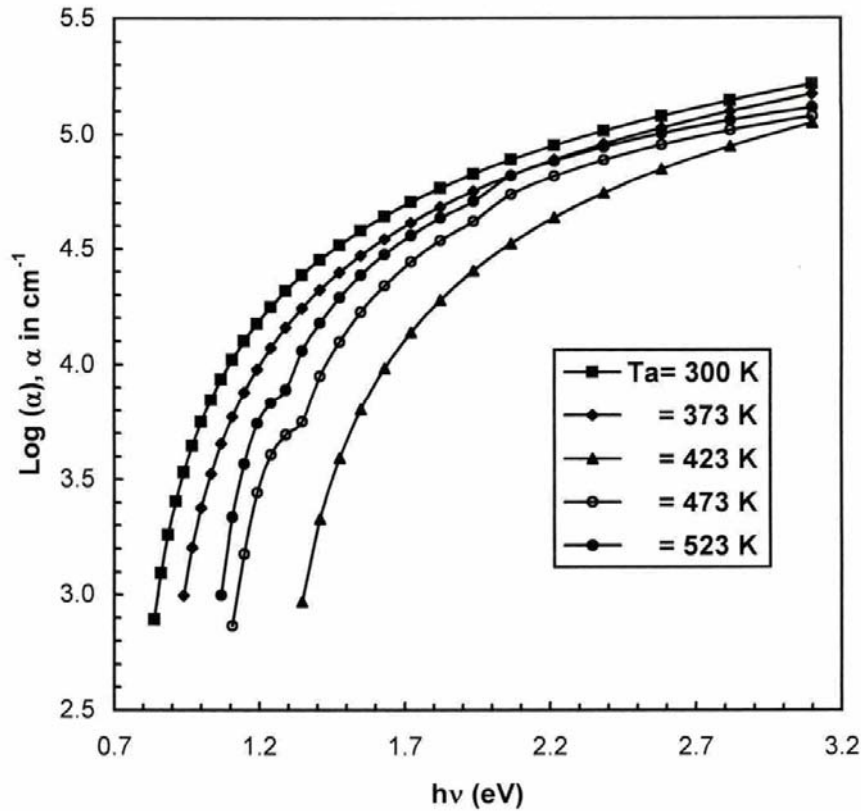


Fig. (5): Optical absorption spectra for the as-deposited and annealed films of $\text{AgGa}_{0.5}\text{In}_{0.5}\text{Te}_2$.

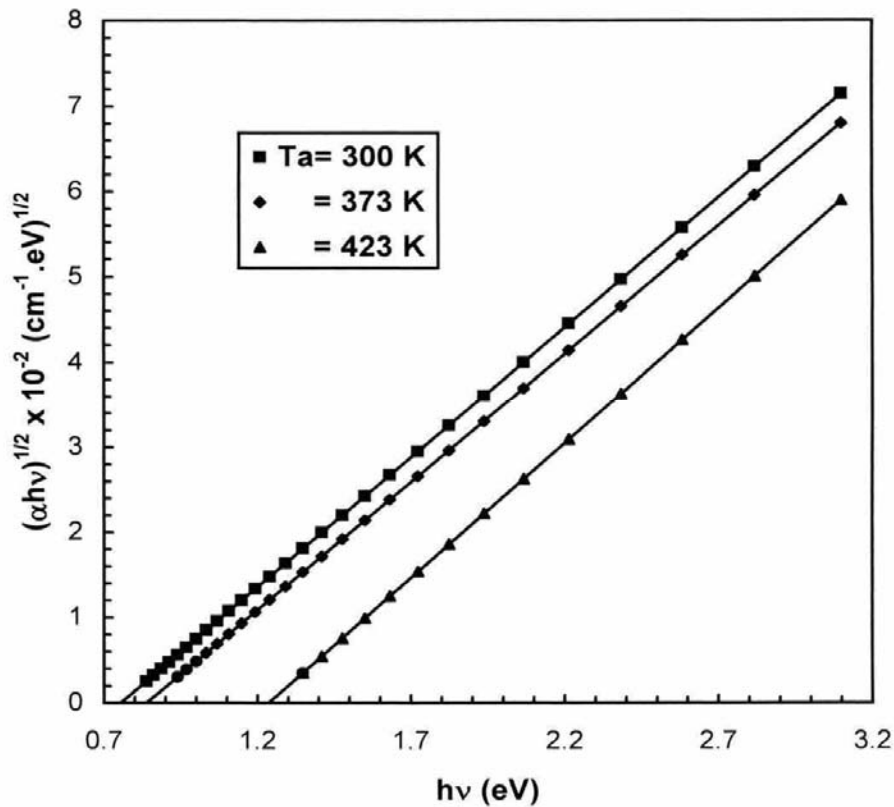


Fig. (6): Plot of $(\alpha h\nu)^{1/2}$ against $h\nu$ for $\text{AgGa}_{0.5}\text{In}_{0.5}\text{Te}_2$ amorphous films.

The analysis of the absorption coefficient of the crystalline films (Fig. 5) annealed at $T_a = 473$ and 523 K shows that the rise of α in the photon energy range $h\nu \leq 1.35$ and 1.3 eV follows the relation (5) with $p = 1/2$ [12, 16]; with an energy gap $E_{g1} = 1.156$ and 1.117 eV; respectively (Fig.7). This transition corresponds to an allowed direct transition from the top of the valence band to the conduction band minimum at the center of the Brillouin zone. However, on calculating α_1 , using A_1 and E_{g1} determined from Fig. (7) for energies above 1.35 and 1.3 eV, it was found that α_1 is considerably smaller than the absorption coefficient, α , measured experimentally, indicating the existence of additional absorption, $\alpha_2 (= \alpha - \alpha_1)$.

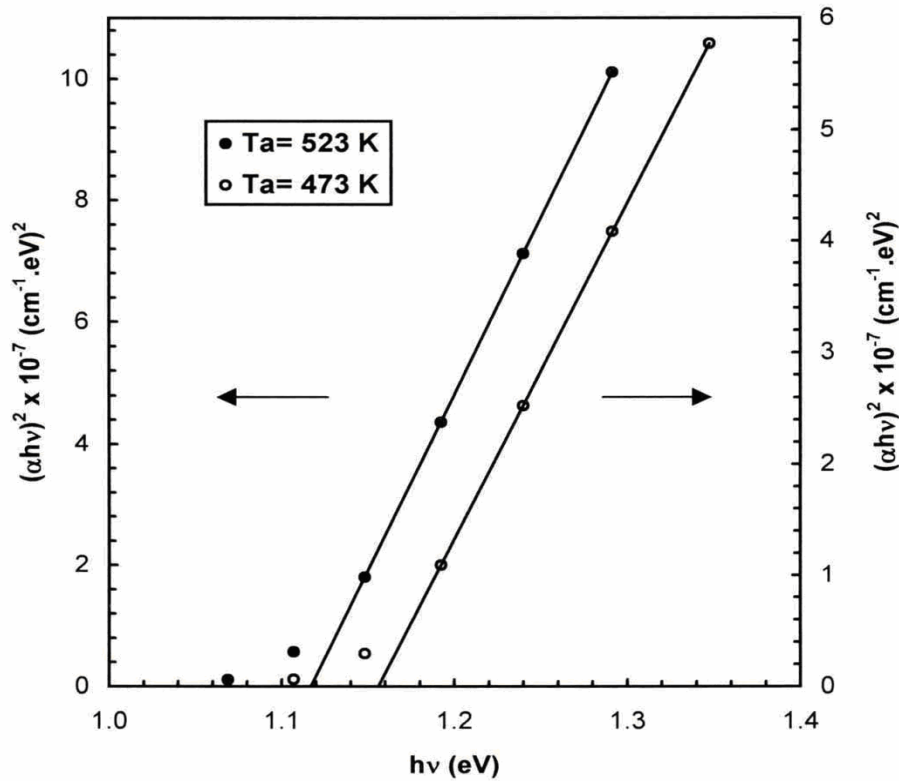


Fig. (7): Plot of $(\alpha h\nu)^2$ against $h\nu$ for $\text{AgGa}_{0.5}\text{In}_{0.5}\text{Te}_2$ crystalline films.

The analysis of the additional absorption coefficient, showed that the dependence of α_2 on $h\nu$ could be described by the relation (5) with $p=3/2$ [12, 16] up to photon energies of about 1.93 eV, with a gap energy $E_{g2} = 1.316$ and 1.255 eV for films annealed at $T_a = 473$ and 523 K, respectively (Fig. 8). This transition corresponds to a forbidden direct transition from the crystal-field-split valence band to the conduction band minimum [17]. Calculating α_2 beyond 1.93 eV and adding $(\alpha_1 + \alpha_2)$ results in a deviation from α , indicating the presence of another higher energy transition.

In the region beyond 1.93 eV, $\alpha_3 = \alpha - (\alpha_1 + \alpha_2)$, followed the relation (5) [12, 16] with $p=1/2$ with a gap energy $E_{g3} = 1.99$ and 1.93 eV for films annealed at $T_a = 473$ and 523 K; respectively (Fig. 8). This transition corresponds to an allowed direct transition from the spin-orbit-split valence band to the conduction band minimum [15]. Calculating $\alpha_c (= \alpha_1 + \alpha_2 + \alpha_3)$ and comparing it with the experimental values of α (α_c), it was found that no further absorption occurs.

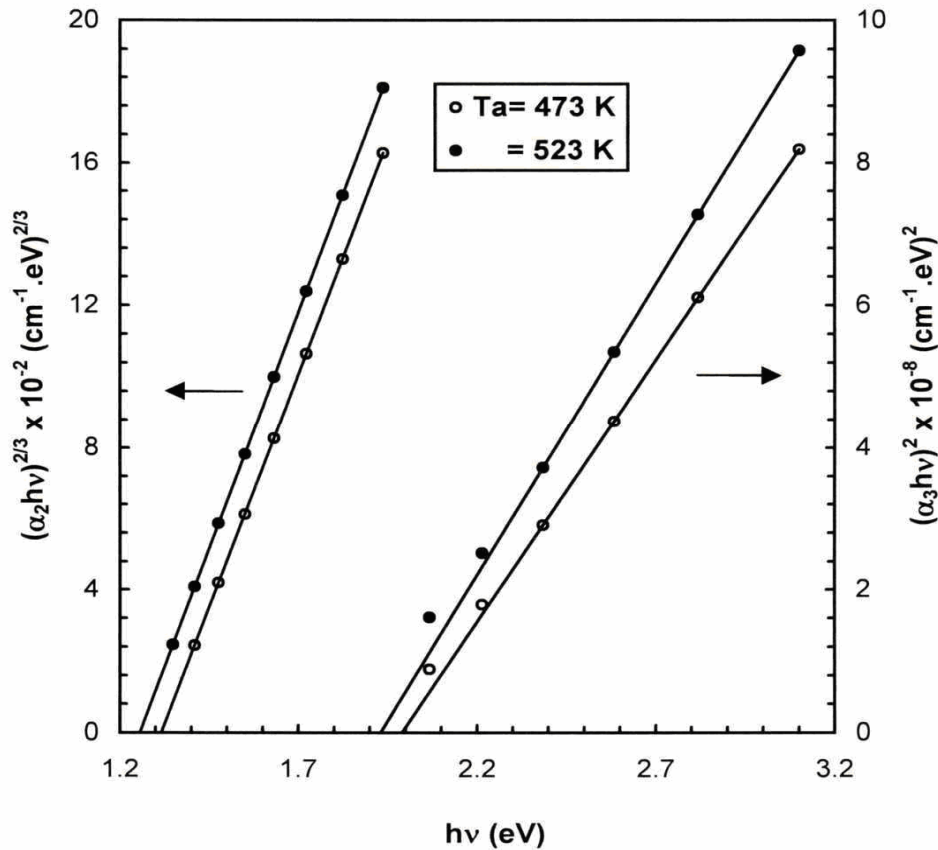


Fig. (8): Plots of $(\alpha_2 h\nu)^{2/3}$ and $(\alpha_3 h\nu)^2$ against $h\nu$ for $\text{AgGa}_{0.5}\text{In}_{0.5}\text{Te}_2$ crystalline films.

From the above analysis, three characteristic band gaps (E_{g1} , E_{g2} , & E_{g3}) were determined for the polycrystalline $\text{AgGa}_{0.5}\text{In}_{0.5}\text{Te}_2$ thin films annealed at $T_a = 473$ and 523 K , which may be attributed to the optical transitions from the valence sub-bands to the conduction band minimum.

The influence of the annealing temperature on the optical parameters (ϵ_∞ , N/m and E_g) of $\text{AgGa}_{0.5}\text{In}_{0.5}\text{Te}_2$ films is shown in Fig. (9) and their determined values are given in Table (2). The dependence of the fundamental optical transition energy, E_g , on the annealing temperature (Fig. 9) revealed that such energy increases on increasing the annealing temperature for as-deposited films and starts to decrease with increasing temperature above 423 K . The increase in the band gap energy, E_g , with annealing temperature $\leq 423 \text{ K}$ may be explained as a result of decrease in the degree of the disorder in the structure

of the deposited films which reflects an increasing in the number of unsaturated bonds. These are turn reduces the localized energy level concentration; hence reflect an increase in the optical band gap. However, for further increasing of the annealing temperature > 423 K, high concentration of localized energy level were achieve causing a decrease in the number of unsaturated bonds. The presence of a high concentration of localized states may be responsible for the decrease of the optical band gap.

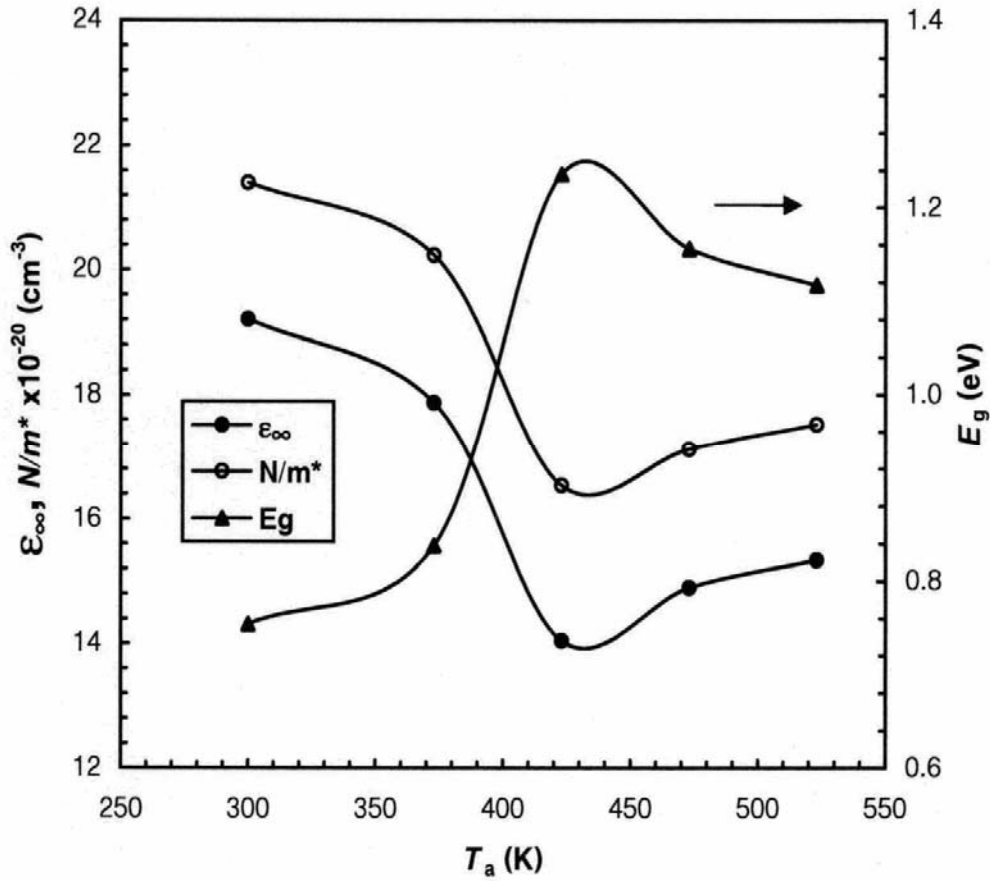


Fig. (9): Dependence of the optical parameters (ϵ_{∞} , N/m and E_g) of $\text{AgGa}_{0.5}\text{In}_{0.5}\text{Te}_2$ films on the annealing temperature.

4. Conclusions:

AgGa_{0.5}In_{0.5}Te₂ films show an amorphous-to-crystalline transition at temperature, $T_a \approx 473$ K. The optical constants (n , k) for both the amorphous and crystalline AgGa_{0.5}In_{0.5}Te₂ films were determined from the transmittance and the reflectance data. The high frequency dielectric constant and the carrier concentration to the effective mass ratio were determined from the analysis of the refractive index at long wavelengths. The analysis of the optical absorption spectra revealed a non-direct optical transition for the amorphous films. While for the polycrystalline films the analysis of the optical absorption spectra revealed three optical transitions, which were attributed to the fundamental, band splitting by crystal-field and spin-orbit effects, respectively. The annealing temperature dependence of the fundamental optical transition energy revealed that such energy increases on increasing the annealing temperature for as-deposited films up to 423 K and starts to decrease with increasing annealing temperature.

References:

1. J. Loferski et al., Conference Records of the 15th IEEE Photovoltaic Specialists Conference (IEEE, New York, 1981) p. 1277.
2. L. L. Kasmerski and S. Wagner, in: Current Topics in Photovoltaics (Academic Press, New York, 1985).
3. I. V. Bondar', V. F. Gremenok, I. A. Viktorov, and O. N. Obraztsova, *J. Appl. Spectrosc.* **64**, 809 (1997).
4. Basumati H. Patel, *Cryst. Res. Technol.* **30**, 195 (1995).
5. R. Shukla, P. Khurana, and K. K. Srivastava, *J. Mater. Sci. – Mater. Electron.* **3**, 132 (1992).
6. I. V. Bondar', V. F. Gremenok, O. N. Obraztsova, L. V. Rusak, V. Yu. Rud', and Yu V. Rud', *J. Appl. Spectrosc.* **66**, 151 (1999).
7. M. C. Ohmer, J. T. Goldstein, D. E. Zelmon, A. W. Saxler, S. M. Hegde, J. D. Wolf, P. G. Schunemann, and T. M. Pollak, *J. Appl. Phys.* **86**, 94 (1999).
8. E. A. El-Sayad, *Phys. Stat. Sol. (a)* **201**, 103 (2004).
9. S. Tolansky, in: "Multiple – Beam Interference Microscopy of Metals", (Academic Press, London, p. 55 (1970).
10. A. M. Salem, W.Z. Sliman, Kh. A. Mady; *physica B* **48**, 2258 (2007).
11. G. Kanellis, C. Kambas, J. Spyridelis; *Mat. Res. Bull.* **11**, 429 (1976).
12. J. I. Pankove, "Optical Processes in Semiconductors", (Dover Publ. Inc, New York, p. 103 (1971).
13. T. S. Moss, G. J. Burrell, and B. Ellis, in "Semiconductor Optoelectronics", (Butterworths London, p. 10, 19 (1973).
14. W. G. Spitzer and N. Y. Fan, *Phys. Rev.* **106**, 882 (1957).

- 15.** J. Tauc, in: “*Amorphous and Liquid Semiconductors* “, (Plenum, New York, 1974) Ch. 4.
- 16.** F. Bassani and G. P. Parravicini, in: *Electronic States and Optical Transitions in Solids* (Pergamon Press, Oxford, 1975).
- 17.** L. Artus, Y. Bertrand, and C. Ance, *J. Phys. C* **19**, 5937 (1986).